Passive and active scalar transport phenomena in low Mach number flows

Guillermo Araya^{a)}

Computational Turbulence and Visualization Lab, Dept. of Mechanical Eng., University of Texas at San Antonio, TX 78249, USA

a)Corresponding author: araya@mailaps.org

Abstract. Direct Numerical Simulation (DNS) of spatially-developing turbulent boundary layers (SDTBL) is performed over isothermal/adiabatic flat plates for incompressible and compressible-subsonic ($M_{\infty} = 0.5$ and 0.8) flow regimes. Similar low Reynolds numbers are considered in all cases with the purpose of assessing modest flow compressibility on low/high order flow statistics of Zero Pressure Gradient (ZPG) flows. The considered molecular Prandtl number is 0.72. Additionally, temperature is regarded as a passive scalar in the incompressible SDTBL with the purpose to examine differences in the thermal transport phenomena of subsonic flows, i.e., passive vs. active scalar. It was found that the Van Driest transform and Morkovin scaling are able to collapse incompressible and subsonic quantities very well.

INTRODUCTION

The transport of scalar fields in turbulent boundary layer is a typical physical phenomenon in fluid dynamics. An active scalar changes the physical fluid properties, such as density and viscosity, according to the local scalar concentration. Examples of active scalars can be found in research areas such as magnetohydrodynamics, natural convection and Navier-Stokes with Eckman friction [1, 2]. In active scalar transport there are two-way coupling (fluid-scalar), and Lagrangian trajectories are coupled with the scalar forcing [1]. A passive scalar (tracer), on the other hand, does not affect the thermodynamic and transport properties of the fluid; nevertheless, there is still a transport equation to be solved. Furthermore, a passive scalar is defined as a diffusive contaminant that exists in such a low concentration in a flow that it has no effect on the dynamics of the fluid motion, Warhaft [3]. However, that low concentration of passive scalar is sufficient to cause a significant impact on energy expenditures, air pollution and design of chemical processes. The turbulent transport of passive scalars is crucial in many industrial applications of technological importance, such as heat transfer in electronic/mechanical devices, chemicals dissolved in gases, contaminant/humidity dispersed in atmospheric flow, to name a few.

In general, active and passive scalars have been analyzed and contrasted in incompressible flows. Celani *et al.* [4] focused on the problem of relating the Eulerian properties to the Lagrangian ones in the transport phenomena of active scalar. Frisch *et al.* [5] proposed a Lagrangian method to compute multiple correlations in passive scalar convection. In terms of compressible flows, experimental knowledge was documented on subsonic and supersonic turbulent boundary layers, mostly by inspecting scaling laws with respect to Reynolds and Mach number effects [6]. A DNS study over subsonic adiabatic SDTBL for $M_{\infty} = 0.3$, 0.5, 0.7 and 0.85 was performed by [7] with the following mesh resolution at $M_{\infty} = 0.85$: 18.4-15.1, 0.69-0.57 and 6-4.9 along the streamwise, first off wall-normal and spanwise directions, respectively. Additionally, compressible turbulent flow in a circular pipe was carried out by [8] at bulk Mach numbers between 0.2 to 3. According to [9], compressibility effects on the wall shear stress were non-negligible even at low Mach numbers (around 0.3) based on experiments performed over compressible pipe flows.

In all above mentioned references [7, 8], the full compressible Navier-Stokes equations for a perfect shock-free heat-conducting gas (equation of state) were solved, including low Mach number cases around 0.2-0.3. Furthermore, low-Mach formulations assume a linear expansion for the thermodynamics variables so that one can use a state equation. In the incompressibility approximation, the pressure does not prevail a thermodynamic variable anymore, taking a "buffer" role in incompressible flow to ensure the zero-divergence condition in the velocity field. Therefore, pressure and velocity are coupled in the continuous domain via the Poisson equation for pressure, which ensures that continuity

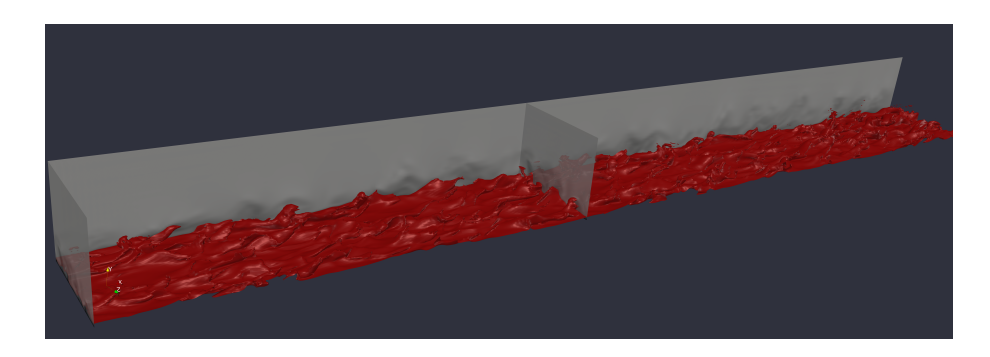


FIGURE 1. Boundary layer schematic for the Mach 0.8 case. Iso-surfaces of instantaneous static temperature (in red), contours of instantaneous temperature in extracted planes (flow from left to right).

TABLE 1 DNC Cons

IABLE I. DNS Cases.						
Case	M_{∞}	T_w/T_∞	$Re_{\delta 2}$	δ^{+}	$L_x \times L_y \times L_z$	$\Delta x^+, \Delta y_{min}^+/\Delta y_{max}^+, \Delta z^+$
Incompressible	0	Isothermal	302-582	144-261	$45\delta_{inl} \times 3.5\delta_{inl} \times 4.3\delta_{inl}$	14.7, 0.2/13, 8
Subsonic	0.5	1.045	300-552	142-254	$42.6\delta_{inl} \times 3\delta_{inl} \times 3\delta_{inl}$	13.8, 0.18/13, 7.6
Subsonic	0.8	1.115	309-571	146-253	$43\delta_{inl} \times 3\delta_{inl} \times 3\delta_{inl}$	14, 0.18/13.4, 7.8

is satisfied. In this study, the temperature effect on first and second order statistics of the fluid velocity field is evaluated for compressible turbulent boundary layers in the low and high subsonic flow regimes via direct simulations of the coupled continuity, Navier-Stokes and energy equations. For an unbiased point of compressibility effect assessment in the subsonic flow regime ($M_{\infty} = 0.5$ and 0.8), DNS of incompressible SDTBL (by solving the Poisson equation for pressure) is taken into account with thermal boundary layer evolution and temperature regarded as a passive scalar.

Numerical Details: Turbulent Inflow Generation and Boundary Conditions

Unsteady three-dimensional simulations of SDTBL via DNS demand high mesh resolution to resolve even the smallest turbulence scales (Kolmogorov and Batchelor scales). Moreover, the computational box must be large enough to appropriately capture the dynamics of the large-scale turbulent motions. Additionally, it requires the prescription of physically sound turbulent inflow conditions to circumvent the space and time consuming laminar-transition computation. We are employing a type of rescaling-recycling technique ([10]) as proposed by [11], and adapted to compressible flow in [12]. The idea is to extract the flow solution (mean and fluctuating flow components) from a downstream plane (called "recycle") and to apply scaling laws to absorb the streamwise non-homogeneous condition, to finally re-inject it at the inlet plane. In Figure 1, it can be seen the streamwise locations of the inlet and downstream recycle plane. The reader can access to more detailed information at [11, 12]. Direct simulations have been carried out via a highly accurate, very efficient, and highly scalable flow solver. PHASTA is an open-source, parallel, hierarchic (2nd to 5th order accurate), adaptive, stabilized (finite-element) transient analysis tool for the solution of compressible [13] or incompressible flows (Jansen [14]). PHASTA has been extensively validated in a suite of DNS under different external conditions [11, 12, 15]. Turning to boundary conditions, at the wall the classical no-slip condition is imposed for all velocity components. An adiabatic wall condition $(T_w/T_r = 1)$ is prescribed for the thermal field with the ratio T_w/T_∞ = 1.045 and 1.115, respectively. Here, T_w is the wall temperature, T_∞ is the freestream temperature and T_r is the recovery or adiabatic temperature. The lateral boundary conditions are handled via periodicity; whereas, freestream values are prescribed on the top surface. Table 1 depicts the characteristics of the evaluated three DNS databases of flat plates in the present study: one incompressible case and two subsonic cases ($M_{\infty} = 0.5$ and 0.8). Numerical details are reproduced here for readers' convenience. The time steps (Δt^+) in wall units were fixed to 0.38, 0.15 and 0.31 for the incompressible, Mach 0.5 and Mach 0.8 runs, respectively. In all cases, the number of mesh points in the streamwise, wall-normal and spanwise direction is $440 \times 60 \times 80$ (roughly a 2.1-million point mesh). The cases were run in 96 cores in HPE SGI 8600-Gaffney (NAVY, DoD).

The most relevant DNS results (due to limited space) are shown. Fig. 2 (a) depicts the time-averaged streamwise velocity profiles in wall units for present DNS. The Van Driest transform is applied in both subsonic cases ($M_{\infty} = 0.5$ and 0.8), which enables absorption of compressibility effects; and, therefore direct comparison with incompressible cases. In addition, external incompressible DNS profiles are included ([16, 17, 18, 19]). Overall, a satisfactory collapse is seen among incomprensible and subsonic cases. Because of the low Reynolds numbers considered, the log region

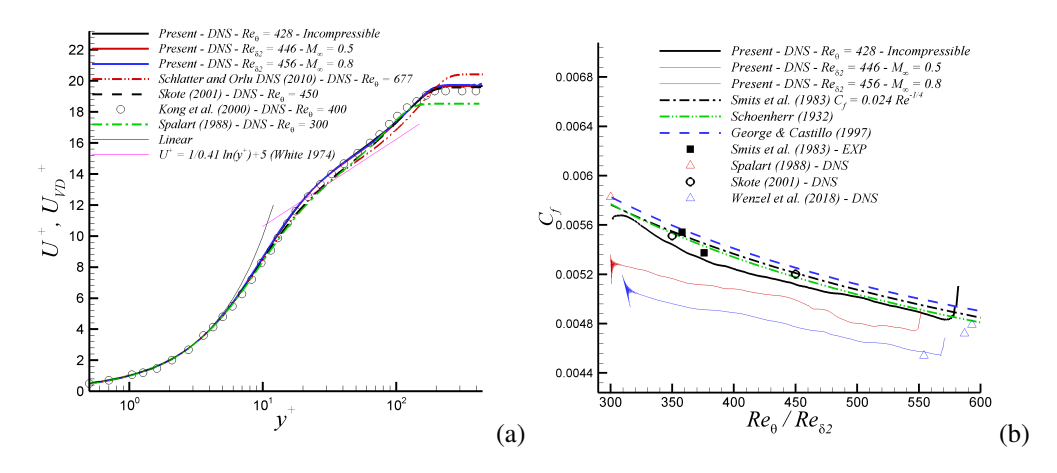


FIGURE 2. (a) Mean streamwise velocity and (b) skin friction coefficient.

seems pretty short, or at a steeper slope. The skin friction coefficients $[C_f = 2(u_\tau/U_\infty)^2\rho_w/\rho_\infty]$ as a function of the momentum thickness Reynolds numbers (Re_θ for incompressible cases and $Re_{\delta 2}$ for compressible cases) are exhibited in fig. 2 (b). As the Mach number increases, the C_f profiles move downward, mostly due to the decrease of the ρ_w/ρ_∞ ratio in adiabatic flat plates, showing somehow similar slopes. Present incompressible C_f values agree quite well with the empirical correlation proposed by Schoenherr for flat plates (particularly by the end of the computational domain), as well as with DNS by [17] and experiments by [20]. Furthermore, DNS data by [7] is included at $M_\infty = 0.3$, 0.5 and 0.85 with decreasing values of C_f , showing a fairly good agreement with present DNS at similar compressibility levels, i.e., Mach numbers. Turbulence intensities and Reynolds shear stresses are depicted by fig. 3 (a) in wall units. The present incompressible DNS results contrast quite well with those of [17] at very similar Reynolds numbers, except in u'^+ peaks with discrepancies in the order of 5%. In subsonic quantities, the Morkovin scaling is implemented to account for wall-normal density variation. While the collapse of present DNS cases (i.e., Incompressible, Mach 0.5 and Mach 0.8) is not absolute (particularly, at peak value locations), the profile affinity is encouraging. Turning to the mean static temperature in compressible flow, the T/T_∞ and U/U_∞ relationship is expressed in terms of the Walz's equation,

$$\frac{T}{T_{\infty}} = \frac{T_w}{T_{\infty}} + \frac{T_r - T_w}{T_{\infty}} \left(\frac{U}{U_{\infty}}\right) - r\frac{\gamma - 1}{2} M_{\infty}^2 \left(\frac{U}{U_{\infty}}\right)^2 \tag{1}$$

where r is the recovery factor (= $Pr^{1/3}$) and T_r the well known recovery temperature. Figure 3 (b) shows the mean static temperature vs. mean streamwise velocity both normalized by the corresponding freestream value. Overall, the Walz equation gives excellent predictions for the adiabatic subsonic flat plates, backing present DNS of active scalars. Fig. 4 shows the wall-normal turbulent fluxes for incompressible and subsonic cases normalized by freestream values (U_{∞} and T_{∞}). All profiles peak at approximately one-fourth of the boundary layer thickness; however, the normalized values are significantly much larger for the incompressible case according to the selected scales. This can be explained by the fact that the freestream product $U_{\infty}T_{\infty}$ is substantially bigger in the subsonic regimes.

Final Remarks

DNS of turbulent thermal boundary layers is performed. The incompressible flow regime (temperature as a passive scalar) is compared to the subsonic regime (temperature affecting the momentum transport and viscosity). Overall, the Van Driest transform and Morkovin scaling have been able to absorb compressibility effects reasonably well. Future work involves coherent structure analysis inside momentum and thermal boundary layers.

Acknowledgment

This research was funded by the National Science Foundation under grants #2314303 and #1847241. This material is based on research sponsored by the Air Force Office of Scientific Research (AFOSR) under agreement number FA9550-23-1-0241. This work was supported in part by a grant from the DoD High-Performance Computing Modernization Program (HPCMP).

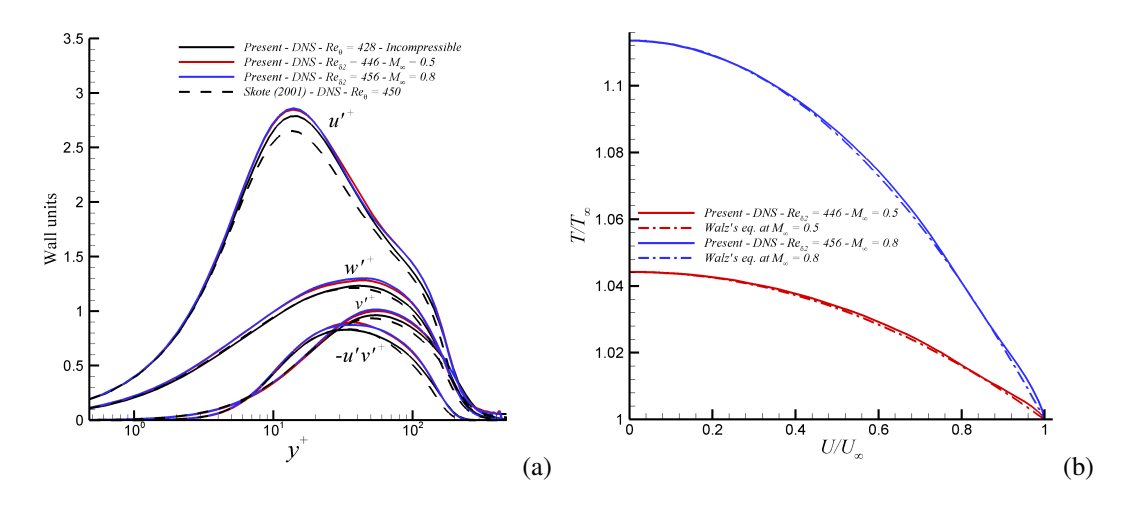


FIGURE 3. (a) Turbulence intensities and Reynolds shear stresses, and (b) mean static temperature.

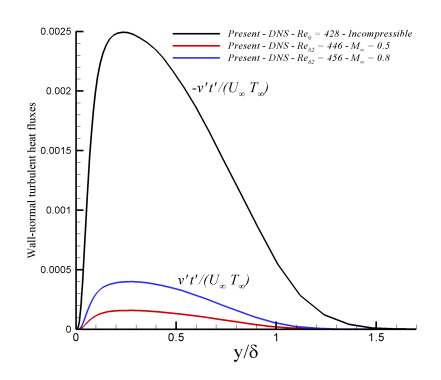


FIGURE 4. Wall-normal turbulent heat fluxes in outer units.

REFERENCES

- [1] A. Celani, T. Matsumoto, A. Mazzino, and M. Vergassola, Phys. Rev. Letters 88, p. 054503 (2002).
- [2] I. Held, R. Pierrehumbert, S. Garner, and K. Swanson, Journal of Fluid Mechanics 282, 1–20 (1995).
- [3] Z. Warhaft, Ann. Rev. Fluid Mechanics **32**, 203–240 (2000).
- [4] A. Celani, M. Cencini, A. Mazzino, and M. Vergassola, Phys. Rev. Letters 89, p. 234502 (2002).
- [5] U. Frisch, A. Mazzino, A. Noullez, and M. Vergassola, Physics of Fluids 11, 2178–218608 (1999).
- [6] J. Dussauge, H. Fernholz, P. Finley, R. Smith, A. Smits, and E. Spina, AGARDograph, AGARD 335 (1996).
- [7] C. Wenzel, B. Selent, M. Kloker, and U. Rist, Journal of Fluid Mechanics 842, p. 428–468 (2018).
- [8] D. Modesti and S. Pirozzoli, International Journal of Heat and Fluid Flow **76**, 100–112 (2019).
- [9] B. Kjellstroem and S. Hedberg, Nov (1968).
- [10] T. Lund, X. Wu, and K. Squires, Journal of Computational Physics **140**, 233–258 (1998).
- [11] G. Araya, L. Castillo, C. Meneveau, and K. Jansen, Journal of Fluid Mechanics 670, 518–605 (2011).
- [12] G. Araya, C. Lagares, and K. Jansen, AIAA SciTech Forum (AIAA 3247313) Orlando, FL. (2020).
- [13] C. H. Whiting, K. E. Jansen, and S. Dey, Comp. Meth. Appl. Mech. Engng. 192, 5167–5185 (2003).
- [14] K. E. Jansen, Comp. Meth. Appl. Mech. Engng. **174**, 299–317 (1999).
- [15] C. Lagares and G. Araya, Energies **16**, p. 4800 (2023).
- [16] P. Schlatter and R. Orlu, Journal of Fluid Mechanics 659, 116–126 (2010).
- [17] M. Skote, Royal Institute of Technology, Stockholm, Sweden **PhD thesis** (2001).
- [18] H. Kong, H. Choi, and J. Lee, Physics of Fluids 12, 2555–2568 (2000).
- [19] P. Spalart, Journal of Fluid Mechanics **187**, 61–98 (1988).
- [20] A. J. Smits, N. Matheson, and P. N. Joubert, Journal of Ship Research 27, 147–15709 (1983).